arXiv:cond-mat/0307113v1 [cond-mat.mes-hall] 4 Jul 2003

# Spectroscopy of soft modes and quantum phase transitions in coupled electron bilayers

S. Luin, [a,c,*] I. Dujovne, [b,c] V. Pellegrini, [a] A. Pinczuk, [b,c,d] B.S. Dennis, [c] A.S. Plaut, [e] L.N. Pfeiffer, [c] K.W. West, [c] J.H. Xu [a]

[a] *NEST-INFM and Scuola Normale Superiore, Pisa I-56126 Italy*
[b] *Dept. of Applied Physics and Applied Mathematics , Columbia University, New York, NY 10027, USA*
[c] *Bell laboratories, Lucent Technologies, Murray Hill, NJ 07974, USA*
[d] *Dept. of Physics, Columbia University, New York, NY 10027, USA*
[e] *Dept. of Physics, Exeter University, Exeter, UK*

**Abstract**

Strongly-correlated two-dimensional electrons in coupled semiconductor bilayers display remarkable broken symmetry many-body states under accessible and controllable experimental conditions. In the cases of continuous quantum phase transitions soft collective modes drive the transformations that link distinct ground states of the electron double layers. In this paper we consider results showing that resonant inelastic light scattering methods detect soft collective modes of the double layers and probe their evolution with temperature and magnetic field. The light scattering experiments offer venues of research of fundamental interactions and continuous quantum phase transitions in low-dimensional electron liquids.

*Key words:* Quantum Hall effect, light scattering, coupled bilayers
*PACS:* 73.43.Lp, 78.30.-j, 73.21.-b

## 1. Introduction

The energy $\Delta$ of the lowest excitation above the quantum ground state represents a characteristic scale for the quantum transformations in the ground states of strongly-correlated low-dimensional electron systems at *zero temperature*. In continuous quantum phase transitions (QPTs), $\Delta$ tends to zero when the critical point of the phase transformation is approached. The collapse of $\Delta$ at the critical point is associated with a diverging characteristic length scale giving rise to specific scaling laws and universal exponents that are explored experimentally. Significant examples are the scaling behavior of the resistivity in quantum Hall regimes [1], and of the conductance in semiconductor quantum dots in the Kondo regime [2].

Several material systems exhibit continuous QPT that are under current intense investigation [3]. The two-dimensional electron systems in semiconductor quantum structures display complex phase diagrams linked to QPTs. Quantization of in-plane kinetic energy into massively degenerate Landau levels in the quantum Hall regimes create ideal environments where QPTs can be induced and studied under controlled experimental conditions. The coupled electron bilayers

* email: s.luin@nest.sns.it; phone ++39-050 509429; fax ++39-050 509417

realized in wide quantum wells or in coupled double quantum wells (DQW) display diverse groups of broken-symmetry states that are linked by QPTs [4]. The richness of the phase diagram of bilayer systems, due to the interplay between intra- and inter-layer Coulomb interactions, has led to the discovery of some of the most intriguing behaviors in contemporary condensed-matter physics [5].

In electron double layers different QPTs can be induced at zero Kelvin by changing the ratio between bare Zeeman energies $E_z$ and tunnelling gaps $\Delta_{SAS}$, where the $\Delta_{SAS}$ are the spacings between the lowest symmetric and antisymmetric levels of the electron bilayers. Additional tuning of the bilayer phase diagram is achieved by changes in the total electron density, the distance $d$ between the layers and the in-plane component of the magnetic field [4,6,7,8,9]. The relevant low-lying (or soft mode) excitations are here charge- or spin-collective modes associated with transitions across the tunnelling gap of the double-layer system. The mode energies have characteristic dispersions that are determined by the electron interactions. Excitonic Coulomb interactions (or vertex-correction terms) of the neutral quasiparticle-quasihole pairs in the transitions are responsible for minima in the dispersion that occur at zero or finite in-plane wavevectors $\mathbf{q}$.

Inelastic light scattering results presented here highlight collective mode softening due to excitonic Coulomb interactions. The mode softening may drive instabilities in the electron bilayers. Direct access to soft excitations by inelastic scattering methods offers powerful venues for probing the physics of QPTs in strongly-correlated systems. We discuss here results of inelastic light scattering experiments that probe soft collective modes in the bilayer electron gas. The experiments uncover direct links between mode softening and excitonic interactions. These soft collective modes, while observed in the symmetric phases, seem to be associated with the emergence of broken-symmetry states in the electron bilayers. These experiments, however, are very challenging. We recall that the observation of soft collective excitations at the superfluid transition in $^4$He by inelastic neutron scattering [10] is one of the few examples reported in the literature.

The modulation-doped DQWs studied in our experiments were grown by molecular beam epitaxy. They consist of two nominally identical GaAs quantum wells of width $d_w$=18 nm separated either by $Al_{0.2}Ga_{0.8}As$ or $Al_{0.1}Ga_{0.9}As$ barriers with width ranging from $d_B$ = 4 nm to $d_B$ = 8 nm. Si $\delta$-doped layers grown both above and below the DQW create two equivalent two-dimensional electron gases (2DEGs). The combined total carrier concentrations used in the experiments reported in this paper are in the range $0.15 \times 10^{11}\mathrm{cm}^{-2} < \mathrm{n} < 1.7 \times 10^{11}\mathrm{cm}^{-2}$ and low-temperature mobilities $0.2 - 1.5 \times 10^6\mathrm{cm}^2/\mathrm{V}s$. Resonant inelastic light scattering spectra were obtained in a conventional backscattering geometry at temperatures between 1.7K and 50 mK using a dye laser tuned to the optical transitions of the GaAs quantum wells. Discussions on fundamentals of resonant inelastic light scattering processes by collective excitations, matrix elements, resonant enhancements and conservation laws can be found in Refs. [6,11,12,13]. Magnetic fields $B_T$ are applied at angles $\theta$ with the normal to the bilayers. The perpendicular component of the field is $B = B_T \cos\theta$.

In Section 2 we review the results at $B$=0 that set up a conceptual and practical framework for studies of unstable $\mathbf{q} = 0$ spin excitation modes at filling factor $\nu = 2$. In Section 3 we consider recent results obtained in the vicinity of $\nu = 2$ at temperatures below 100mK that support the notion that a $\mathbf{q} = 0$ spin soft-mode drives a QPT in electron bilayers. In Section 4 we discuss the most recent experiments at total filling factor $\nu = 1$. These results show that the light scattering experiments provide evidence of soft tunnelling charge-density excitations at finite $\mathbf{q}$ (soft magneto-rotons) in close proximity to the compressible-incompressible phase boundary.

## 2. Coupled bilayers at B=0

Soft-mode driven QPTs were predicted to occur at $B$=0 [7]. In these theories, the instability is caused by a vertex-correction driven softening of the $\mathbf{q}$=0 spin-density tunnelling excitation (SDE) across the two lowest subbands represented by the $\Delta_{SAS}$ gap. At zero magnetic field this excitation is a degenerate triplet characterized by changes of $\delta S_z = \pm 1$ and $\delta S_z = 0$ in spin angular momentum along the normal to the bilayers . The impact of the vertex correction is readily seen in the expression for the mode energy [14]

$$\omega_{SDE}^2 = \Delta_{SAS}^2 - 2(n_S - n_{AS})\,\beta\,\Delta_{SAS}, \qquad (1)$$

where $n_S$ and $n_{AS}$ are the populations of the sym ric and antisymmetric subbands. The factor $(n_S - n$ takes into account the reduction in available p space when two subbands are occupied. The se term in the right-side of Eq. (1) represents the excit binding and the factor $\beta$ parametrizes the stre of vertex corrections. When this intrawell excit term is larger than the interwell couplings represe by $\Delta_{SAS}$, the $\mathbf{q}$=0 SDE collapses. The possible tence of such unstable spin-density excitations sug the emergence of broken-symmetry phases of antif magnetically correlated 2D layers. The time-depen local-density approximation (TDLDA) results of [7] predict a phase transition for electron densities low $0.5\times10^{11}\mathrm{cm}^{-2}$.

In this section we present the results of a com hensive search for the soft $\mathbf{q}$=0 intersubband SDI zero magnetic field. While this work demonstrate absence of such instabilities, it provides the frame for the design and interpretation of the experim at non-zero magnetic fields presented in the next tion. Resonant inelastic light-scattering measurem of the SDE modes have been carried out on a larg of GaAs DQWs of various well shapes, and with tron densities down to $10^{10}\mathrm{cm}^{-2}$. The sample pa eters were chosen to overlap those for which TDI calculations indicate the existence of an unstable that triggers transitions to broken-symmetry pha

Figure 1 shows typical lowest energy intersubband spectra. For $\mathbf{q}\simeq0$, the energy of the single-particle excitations (SPE) equals that of $\Delta_{SAS}$. The highest energy peak arises from the CDE. The CDE energy is given by [14]

$$\omega_{CDE}^2 = \omega_{SDE}^2 + 2(n_S - n_{AS})\,\alpha\,\Delta_{SAS} \qquad (2)$$

where $\alpha$ is the depolarization shift due to direct terms of Coulomb interactions. Usually $\alpha > \beta$, so that the CDE appears higher in energy than both the SPE and SDE [14]. The collective SDE and CDE display well-defined polarization selection rules. SDE are active in depolarized spectra, where incident and scattered light polarizations are perpendicular and CDE occur in polarized spectra measured with parallel polarizations.

We have measured the energy of the CDE, SDE and SPE modes in a series of samples as a function of carrier concentration. Results are plotted in Fig.2(a). A striking feature of the TDLDA calculation is the vanishing SDE mode energy for electron densities below

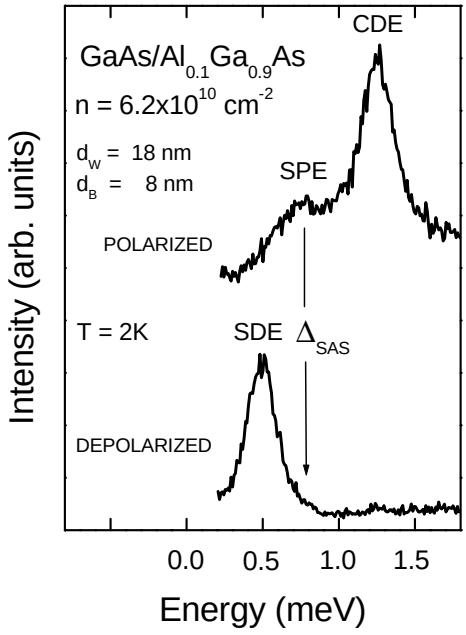


Fig. 1. Inelastic light-scattering spectra of the intersubband excitations of the double quantum well. The peaks of the spin-density excitations (SDE), charge-density excitations (CDE) and single-particle excitations (SPE) are shown. The spectra have been offset for clarity.

$0.5\times10^{11}\mathrm{cm}^{-2}$ [7]. This prediction of the LDA is absent in the experimental results of Fig. 2a.

Other features predicted by LDA calculations are observed experimentally. We find good agreement between the experimental and the LDA values of SPE and CDE energies. The experimental SPE energies show the upward trend with decreasing electron density expected from the renormalized $\Delta_{SAS}$ calculated self-consistently within LDA [15]. In addition, LDA calculations predict that at n<$10^{10}\mathrm{cm}^{-2}$ the excitonic vertex correction should become larger than the depolarization shift resulting in the energy of the CDE falling below that of the SPE [16,17]. And indeed, in the experimental data a similar decrease in the CDE energy is observed as n approaches $10^{10}\mathrm{cm}^{-2}$. As will be seen below, this is due to a decrease in the depolarization shift rather than an increase in the excitonic shift, which is again in qualitative agreement with LDA theory [16].

To obtain further insight into the many-body interactions we can rewrite Eqs. (1) and (2) to determine the direct and exchange terms of the Coulomb interaction: The depolarization shift, $(n_S - n_{AS})\alpha$, and the ex-

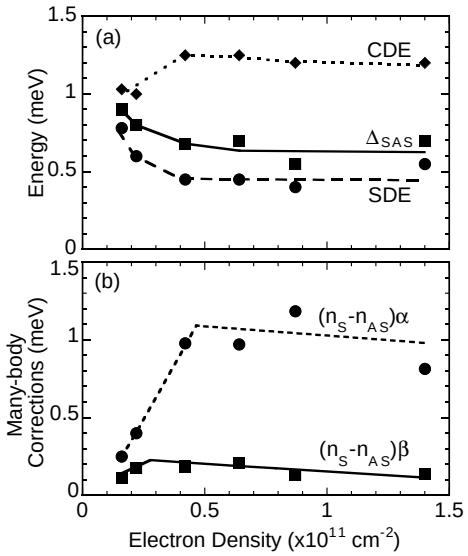


Fig. 2. The measured two-dimensional electron density dependence of (a) the intersubband charge-density excitation energy $\omega_{CDE}$ (dotted), spin-density excitation energy $\omega_{SDE}$ (dashed) and single-particle excitation energy $\Delta_{SAS}$ (solid); and (b) $(n_S - n_{AS})\alpha$ (dashed), and $(n_S - n_{AS})\beta$ (solid), for the GaAs/$Al_{0.1}Ga_{0.9}$As double quantum well structures. The lines are guides to the eye.

citonic shift, $(n_S - n_{AS})\beta$, derived from the measured mode energies shown in Fig. 2a, are plotted in Figure 2b. LDA calculations [18] predict that $(n_S - n_{AS})\alpha$ increases slightly with decreasing n and then drops sharply for electron densities below 0.2 x $10^{11}$cm$^{-2}$. The maximum corresponds to the density at which the second subband just becomes occupied. In Figure 2b, we do indeed observe this behaviour experimentally. Thus the LDA seems to work well when describing the depolarization shift down to very low electron densities.

A different situation prevails in the case of the vertex-correction $(n_S - n_{AS})\beta$ because here we find significant quantitative differences between experiment and LDA theory: For electron densities below 0.5 x $10^{11}$cm$^{-2}$ the experimental values of $(n_S - n_{AS})\beta$ are 2 −5 times smaller than the LDA would predict, with the most significant discrepancies occurring at densities below 0.2 x $10^{11}$cm$^{-2}$, close to the onset of occupation of the antisymmetric state.

Thus, TDLDA is not successful at describing the observed behaviour of both the vertex-corrections and the SDE mode energies at very low density. We attribute these discrepancies, between experiment and LDA theory, to shortcomings of the TDLDA calculation at low densities, when local-density approximations become unreliable because very dilute electron gases can no longer be considered homogeneous even on a local scale. On the other hand, a non-local approach, that treats the exchange Coulomb interaction by means of a variational solution of the Bethe-Salpeter equation in the ladder approximation [19,18], yields predictions for the energies of intersubband collective modes in the DQW that are in good agreement with experiment.

The absence of zero-field enhancements of the vertex-correction $(n_S - n_{AS})\beta$, determined experimentally, indicates that at zero field, and at small values of $\Delta_{SAS}$, the effective electron density, given by $(n_S - n_{AS})$, is limited by the occupation of the antisymmetric state. However, these results are intriguing because, as described below, pronounced softenings of low-energy $\mathbf{q}$=0 SDE, in general agreement with Eq. (1), are seen in spectra from DQWs in perpendicular magnetic fields at even values of $\nu$. Our understanding of this is that the softenings of the spin-density mode in perpendicular field, described below, are due to changes in the effective density of electrons that contribute to the intersubband collective excitations. This effective density can be changed by magnetic field, and for filling factor $\nu$=2 and lower all the electrons can and do contribute.

## 3. Coupled bilayers at $\nu = 2$

At this even-integer value of Landau level filling factor, the spin configuration depends on the relationship between $E_z = g\mu_B B_T$ and $\Delta_{SAS}$ ($g \approx -0.44$ is the gyromagnetic factor and $\mu_B$ is the Bohr magneton), in conjunction with changes in available phase space for the tunnelling intersubband transitions at $\nu = 2$. There are two possible configurations of spin (see Fig. 3). A spin-singlet quantum Hall paramagnet (phase U) is obtained when the electrons occupy the lowest spin-split symmetric levels. In this configuration the spin polarization is zero and the lowest-energy spin transitions are spin-flip (SF) and SDE modes across $\Delta_{SAS}$. Contrary to the $B$=0 case, these excitations are not degenerate under the application of a magnetic field. In the Hartree-Fock framework their energies are $\omega_{SDE}$

for SDE modes and $\omega_{\pm} = \omega_{SDE} - E_z \delta S_z$, $\delta S_z = \pm 1$ for spin-flip (SF) excitations. The other configuration possible is a spin-polarized quantum Hall ferromagnet (phase P). Characteristic excitations in this configuration are spin waves (SW) across the Zeeman gap and SF modes.

The actual spin configuration depends on the strength of the energy required to produce a spin-flip relative to that of the interlayer interactions that enter in the $\Delta_{SAS}$. The energy required to change the orientation of spin incorporates two terms. One is the Zeeman energy $E_z$. The other is the spin stiffness of the 2DEG, given by the increase in Coulomb exchange interaction energy when the spin orientation is changed. Because the spin stiffness has a characteristic $B^{1/2}$-dependence, the spin-singlet configuration prevails at the lower values of $B_T$. The spin-polarized configuration emerges at higher total fields when the spin-flip transition energy in the lowest Landau level is larger than the energy associated with a transition across the tunnelling gap.

Contrary to predictions and experimental observations of first-order phase transitions between phases U and P in single layers [20,21,22], inter-layer interactions in the bilayer systems leads to a novel broken-symmetry intermediate phase D linked to phase U by a continuous second-order phase transition [6,9,23,24]. Under the application of parallel magnetic fields, the ratio between the tunneling and Zeeman gaps can be changed and the system can make transitions from the singlet phase U to the intermediate phase D and at larger parallel fields, to phase P. Signatures of these different configurations of spins were obtained by inelastic light scattering measurements of spin tunneling excitations [6,23]. These works demonstrated that the transition between U and D is associated to the softening of the tunneling SDE. The softening is caused by excitonic interactions that reduce $\omega_{SDE}$ energies to values much lower than $\Delta_{SAS}$ and close to $E_z$ signaling the existence of an unstable SF excitation with $\delta S_z = 1$. In addition to removing the degeneracy of the three spin excitations in the triplet state, the application of the magnetic field allows to manipulate the phase-space factor $(n_S - n_{AS})$. At total filling factor $\nu = 2$ when all the electrons occupy the symmetric states, we have $n_S - n_{AS}$ =n (where n is the total electron density) and all electrons can contribute to the tunnelling transitions [25].

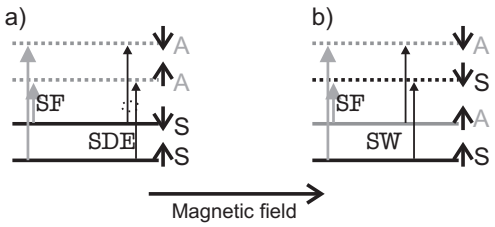


Fig. 3. Schematic representation of the energy level scheme at $\nu$=2. a) In the unpolarized state (phase U), when the symmetric states are populated and b) spin polarized state (phase P), with the lowest symmetric and antisymmetric levels fully occupied. The arrows correspond to the possible excitations in these configurations. SF: spin flip mode; SDE: spin-density excitation; SW: spin wave. The arrows on the side of the levels correspond to spin.

The zero-temperature properties of the ground state in the new intermediate phase have been the subject of intense theoretical investigations [9,26,27,28,29,30]. It is now well accepted that the competition between interlayer tunnelling, Zeeman splitting, intralayer and interlayer Coulomb interactions, leads to a spontaneous symmetry breaking in the bilayer and electron spins in each layer tilted away from the external magnetic field direction (canted phase).

We focus here on the SDE behavior observed under changes of $B_T$ while keeping the filling factor of $\nu = 2$. Detailed analysis of the SDE softening down to T=200mK when the $\nu = 2$ state is approached in a tilted-field configuration indicates that the SDE energy reaches its lower values in the low-field side of $\nu = 2$ (and then disappears for larger values of magnetic field) but at energies significantly larger than $E_z$ (implying a spin-flip mode at energy $\omega_-$ above zero) [6,23]. In order to fully understand these results, it is important to recall that in the T>0 region close to the critical point of QPTs, large thermal population of low energy soft modes cause critical fluctuations that destroy the long-range order of the broken symmetry phase [1]. In the case of the continuous QPT in coupled bilayers at $\nu$=2 this could imply that at T>0, the system become unstable before reaching $\nu$=2 and $\omega_{SDE} = E_z$. This is consistent with results shown in Refs.[6,23]. In a attempt to further validate this picture we have extended the inelastic light scattering measurements at lower temperatures (down to 50mK). At the lowest temperature, the energies are smaller than at 300mK. The fact that the energy approaches $E_z$ when the temperature is lowered provides evidence that the transi-

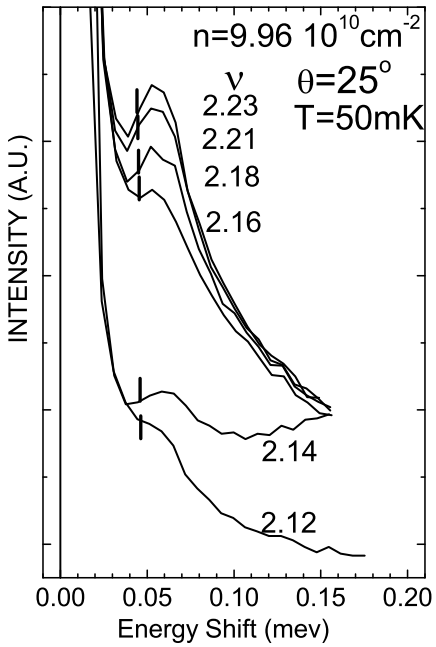


Fig. 4. Typical spectra at different filling factors for $\nu > 2$. Experiments were done at 50mK and a tilt angle of $25^o$. The vertical lines on each spectra correspond to the value of the Zeeman energy.

tion is almost continuous.

Figure 4 shows typical spectra at different filling factors near $\nu$=2 and T=50mK. The sample (a DQW with 8 nm $Al_{0.1}Ga_{0.9}As$ barrier, density of $9.96 \times 10^{10}\mathrm{cm}^{-2}$ and mobility close to $10^6\mathrm{cm}^2/\mathrm{V}s$) is tilted ($25^o$) from the plane perpendicular to the magnetic field. There are two main contributions to these spectra: the sharp peak corresponds to the inelastic light scattering signal due to the SDE, while the broad background is due to photoluminescence.

The impact of temperature changes near $\nu = 2$ is shown in Fig. 5. Previous results [6,23] have demonstrated that at 300mK and at tilt angle of $20^o$ the system is in the spin unpolarized phase, while at $35^o$ the sample is already in the ferromagnetic phase. SDE energies are displayed at different magnetic fields near $\nu = 2$ for 50mK (circles) and 300mK (squares) and at $25^o$. At our lowest temperature attainable, 50mK, the system shows the same type of behavior of the SDE peaks seen at 300mK with same angle, but consistently at lower energies. The excitation softens markedly as the filling factor is diminished (larger magnetic fields), and disappears as it gets closer to $\nu$=2 (vertical line in

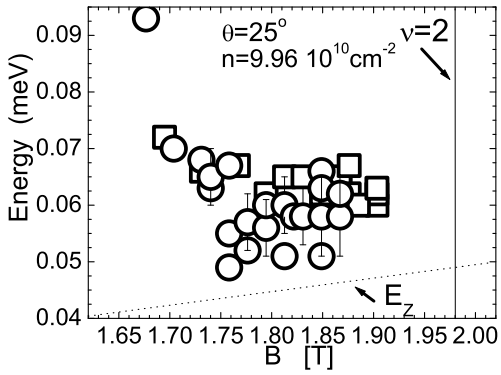


Fig. 5. Magnetic field dependence of the spin-density excitation in the vicinity of $\nu = 2$ at 50mK (◯) and 300mK (□). The experiments were done at a tilt angle of $25^o$. Typical error bars are shown.

Fig. 5). In these regions of magnetic fields the energy of the mode is very close to $E_z$ (see dotted line in Fig. 5). It is possible that the mode becomes overdamped very close to $\nu$=2, and this could explain why the mode is no longer observable at filling factors slightly larger than $\nu$=2, where its energy is comparable to $E_z$. Detailed values of the Zeeman energy $E_z$ are obtained from inelastic light scattering measurements of SW excitations in phase P.

The softening of the intersubband SDE to values close to $E_z$ implies the emergence of spin flip excitations with $\delta S_z$=1 at vanishing small energies that could lead to instabilities in the system. The temperature dependence (down to the lowest temperatures we can achieve) shows that the modes behave in a manner consistent with a QPT at T=0.

## 4. Coupled bilayers at $\nu = 1$

In the previous section we have shown that $\mathbf{q} = 0$ spin tunnelling modes in coupled bilayers can become unstable. Unstable soft modes at finite wavevectors were also predicted to occur in electron-hole systems at strong magnetic fields [31] and in electron bilayers at total filling factor $\nu = 1$ [32,33,34,35,36]. In this section we consider resonant inelastic light scattering studies that probe such excitations.

We recall that the relevant range of in-plane wavevectors ($\mathbf{q}$) accessible to inelastic light scattering experiments is restricted by wavevector conservation

in the scattering process to scattering wavevectors $q$ $\approx 10^5$ cm$^{-1}$. This wavevector range implies access to mode wavevectors $q \leq 0.2 l_B^{-1}$, where $l_B$ is the magnetic length. For this reason the measurements discussed in the previous sections access the long-wavelength limit $\mathbf{q} \rightarrow 0$. The conservation law of wavevector originates from the translational invariance of the 2D system. Even the most perfect samples of 2D electron systems are subject to residual disorder, particularly in the quantum Hall regimes. One of the significant manifestations of residual disorder in resonant inelastic light scattering is the activation of large wavevector collective modes [37,38]. The experiments at $\nu = 1$ take advantage of this feature of light scattering experiments to study soft magnetoroton modes.

A distinct feature of the Hartree- Fock calculations is the magnetoroton minimum at finite wavevectors $q \sim l_B^{-1}$[39]. Magnetoroton excitations were predicted to occur in the dispersions of inter-Landau level modes and in intra-Landau level excitations of the fractional quantum Hall regime [39,40,41]. The minima arise, as mentioned above, from the $q$-dependent excitonic binding in quasiparticle-quasihole pairs.

Observation of roton minima by resonant inelastic light scattering requires breakdown of wavevector conservation assigned to the impact of residual disorder. With absence of wavevector conservation, the light spectra can reveal features of the density of states of Landau level excitations. Massive breakdown of wavevector conservation was indeed invoked to interpret resonant inelastic light scattering experiments in the integer and fractional regimes [37,42,43]. These experiments revealed magnetoroton excitations and excitations with $q \gg l_B^{-1}$.

We have taken advantage of breakdown of wavevector conservation in resonant inelastic light scattering to explore possible links between soft magnetorotons and QPTs in electron bilayer in the quantum Hall regimes [44]. Soft rotons are crucial elements in the theoretical constructions that predict and interpret QPTs in the two-dimensional electron system. One remarkable example is given by the transition to a Wigner crystal state predicted to occur at fractional filling factors beyond 1/7 [40,45]. This link, however, has not yet been addressed in experiments.

The role of soft magnetorotons is particularly intriguing in coupled bilayers at total Landau level filling factor $\nu_T = 1$. At this filling factor value, the bilayer

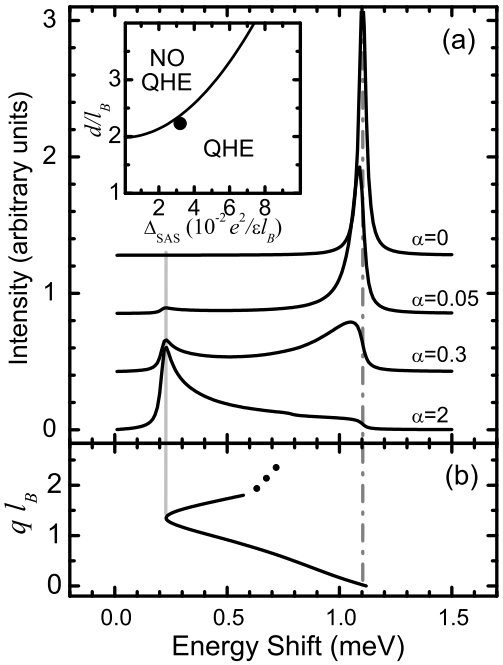


Fig. 6. Panel (a): Calculated inelastic light scattering spectra. $\alpha$ labels the breakdown of wavevector conservation (see text). The curves are the response functions calculated in TDHFA including the wavevector conservation breakdown, using the dispersion shown in panel (b), for a sample close to the phase transition (phase diagram in inset of panel (a))

system displays a rich phase diagram determined by the interplay between single-particle tunnelling gap $\Delta_{SAS}$ with intra- and inter-layer interactions[4]. Two distinct phases were identified on the basis of the value of the longitudinal magneto-resistance measured in magneto-transport experiments. One of the two phases is characterized by the existence of the quantum Hall effect at $\nu_T = 1$ while the other not. The phase diagram is shown in the inset of Fig. 6 [8,46]. In current theories the compressible-incompressible QPT is linked to a roton instability in the CDE across the tunnelling gap [32,33,34,36]. In Hartree-Fock calculations the roton softening instability is due to large excitonic bindings between quasiparticle and quasihole that occurs with a reduction in $\Delta_{SAS}$. In order to show how the breakdown of wavevector conservation can lead to manifestations of collective CDE modes at finite $q$ in the inelastic light scattering spectra we first recall that intensities of inelastic light scattering is in the lowest order approximation proportional to

the dynamic structure factor $S(q,\omega;\alpha)$. Here $\alpha$ is a phenomenological broadening parameter in wavevector space, used to account for the effects of disorder in the breakdown of wavevector conservation. Within this model, used by Marmorkos and Das Sarma [38], we have:

$$S(q,\omega;\alpha) \sim \frac{\alpha}{\pi l_B}\int dq' \frac{S(q',\omega)}{(q-q')^2+\left(\alpha\, l_B^{-1}\right)^2}\,, \qquad (3)$$

where $S(q',\omega)$ is the electronic dynamic structure factor in the translation invariant system. $S(q',\omega)$ for charge-density excitations across the symmetric-antisymmetric gap is given by:

$$S(q,\omega) \propto \frac{|M(q)|^2\,\omega_C(q)\;\omega\Gamma}{\left[\omega^2-\omega_C^2(q)\right]^2+\omega^2\Gamma^2}\,, \qquad (4)$$

where $\Gamma$ is a homogeneous broadening.

To highlight the impact of breakdown of wavevector conservation we focus on a sample in close proximity to the phase boundary (see the dot in the inset of Fig. 6(a)) for which the calculated dispersion is shown in Fig. 6(b). The dispersion is characterized by a deep magnetoroton which anticipates the occurrence of a continuous QPT. We note that TDHFA being a mean-field theory fails to reproduce the collective mode dispersion when $q \gg l_B^{-1}$. That part of the dispersion was not included in the model. Figure 6(a) shows the calculated inelastic light scattering spectra for different values of $\alpha$. In these calculations a broadening factor $\Gamma = 0.035$ meV, due to lifetime limited by disorder and impurity scattering, was considered [38]. Further details on the results of the calculations can be found in Ref.[44]. In Fig. 6(a) we find that small values of $\alpha$, of the order of $0.1 l_o^{-1}$ , are sufficient to yield significant intensity at the energy of magnetoroton critical point in the density of states. This is due to the fact that the matrix element $|M(q)|^2$ that enters the dynamic structure factor and acts as the oscillator strength for inelastic light scattering tends to peak sharply at the magnetoroton wavevector when the bilayer approaches the phase transition instability [44].

In Fig. 7 we compare measured spectra (Fig. 7(a)) with calculations in which $\alpha$ is set at 0.4 (Fig. 7(b)). The sample is characterized by a 7.5-nm-wide $Al_{0.1}Ga_{0.9}As$ barrier, electron density n=1.2 $\times$ $10^{11} cm^{-2}$ and $\Delta_{SAS}$ = 0.32 meV and its position in the phase diagram corresponds to the dot in the inset of Fig. 6. A value of $\alpha = 0.4$ yields an effective

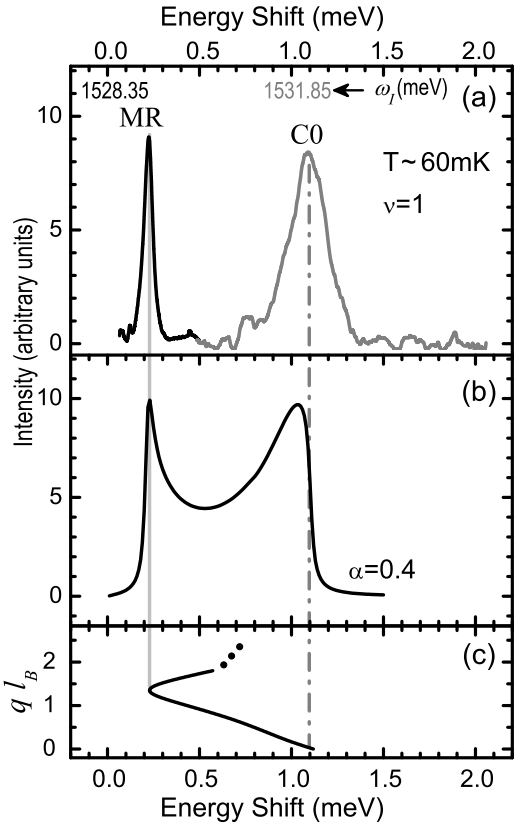


Fig. 7. Comparison within theory and experiment. Panel (a): MR and C0 resonant Raman peaks, for two different incident photon energies (reported in the figure). Background is subtracted. Panel (b): response function for a chosen value of $\alpha$=0.4. (c): collective mode dispersion.

length scale of $\sim 3l_B$ for the terms in the disorder potential responsible for the breakdown of wavevector conservation that interprets the data. The resonant inelastic light scattering spectra are obtained at two different incident photon energies and displayed after conventional subtraction of background due to laser and magneto-luminescence. The assignments of the two spectral features to CDE at $q = 0$ (C0) and to the magneto-roton (MR) are consistent with the calculated dispersion shown in Fig. 6(b) and Fig. 7(c).

The calculation reproduces the energy position and the widths of the peaks. The fact that the C0 width is larger than that of the MR is significant and seems to reflect the peculiar behavior of the $|M(q)|^2$ factor close to the phase boundary. On the contrary, results obtained from a sample far from the phase boundary

show a broad and weak MR peak (compared to C0) and located at higher energies ($\approx 0.6$ meV) [44]. The calculated spectra shown in Fig. 7 differ from the measurements in the region between the C0 and MR modes. The discrepancy could be related to differences in resonant enhancements.

## 5. Conclusions and Perspectives

We have presented extensive results that use light scattering methods to probe soft, unstable, collective excitations in two-dimensional electron systems. Inelastic light scattering has the capability to detect collective soft modes at finite wavevectors as well as spin- or charge-density modes at $\mathbf{q} = 0$ and at $\mathbf{q} = \infty$. Since the latter are the only excitations probed in magneto-transport, light scattering studies have the potential to bring a new wealth of information into studies of quantum phase transitions, spin states and other new broken-symmetry phases in modulation-doped low-dimensional semiconductors. The observations at zero magnetic fields and at total filling factor $\nu = 2$ offer significant examples of the capabilities of this approach. The experiments at $\nu = 2$ are the first to demonstrate mode softening due to excitonic Coulomb interactions in the quantum Hall regime. The experiments at total filling factor $\nu = 1$ are particularly revealing since they offer direct evidence of soft magnetorotons in the quantum Hall regime. These results are significant because they suggest that roton softening plays major roles in the incompressible-compressible phase transitions of the bilayers at $\nu = 1$, and suggest a leading role of excitonic Coulomb interactions in transitions between the highly correlated phases. The results are consistent with a scenario in which the instability is associated with the condensation of neutral excitons, a subject of current interest in bilayers and in other semiconductor systems [47,48,49]. The possible link between exciton condensation and quantum Hall phases in coupled bilayers highlights the role of the quantum Hall regime as a versatile laboratory, almost "magic" in its enormous possibilities, to study quantum liquid phenomena relevant to a multitude of different areas of condensed-matter physics. The liquids of quantum Hall states in semiconductor structures, in fact, can be created and probed in controlled experiments. To this end, it is worth noting the similarities between the magnetoroton observed in the coupled bilayers with the finite-wavevector excitations observed by inelastic neutron scattering in superfluid $^4$He [10] and in the high-$T_c$ superconductor $YBa_2Cu_3O_7$ [50]. These links highlight the impact of experimental and theoretical research on quantum phase transitions and broken-symmetry states in the bilayer electron gas.

## 6. Acknowledgements

These works were supported by the Nanoscale Science and Engineering Initiative of the National Science Foundation under NSF Award Number CHE-0117752, by a research grant of the W. M. Keck Foundation, by CNR (Consiglio Nazionale delle Ricerche), by INFM/E (Istituto Nazionale per la Fisica della Materia, section E), by the Italian Ministry of University and Research (MIUR) and by the Leverhulme Trust (UK).

References

[1] S. L. Sondhi and et. al. *Review of Modern Physics*, 69:315, 1997.

[2] M.A. Kastner and D. Goldhaber-Gordon. *Solid State Comm.*, 119:245, 2001.

[3] S. Sachdev. *Quantum Phase Transitions*. Cambridge University Press, 1999.

[4] S. M. Girvin and A. H. MacDonald. *Perspectives in Quantum Hall Effects, S. Das Sarma and A. Pinczuk editors*, Wiley, New york, Chapter 5:161, 1997.

[5] S. Girvin. *Phys. Today*, page 39, June 2000.

[6] V. Pellegrini and A. Pinczuk. *Solid State Comm.*, 119:301, 2001.

[7] S. Das Sarma and P.I. Tamborenea, Phys. Rev. Lett. **73**, 1971 (1994); R.J. Radtke and S. Das Sarma, Solid State Commum. **96** 215 (1995); Solid State Commum. **98** 771 (1996).

[8] S. Q. Murphy, J. P. Eisenstein, G. S. Boebinger, L. N. Pfeiffer, and K. W. West. *Phys. Rev. Lett.*, 72:728, 1994.

[9] Lian Zheng, R. J. Radtke, and S. Das Sarma. *Phys. Rev. Lett.*, 78:2453, 1997.

[10] E.C. Svensson, W. Montfrooij, and I.M. de Schepper. *Phys. Rev. Lett.*, 77:4398, 1996.

[11] A. Pinczuk. *Perspectives in Quantum Hall Effects, S. Das Sarma and A. Pinczuk editors*, Wiley, New york, Chapter 8:307, 1997.

[12] P. Hawrylak, J. Wu, and J. J. Quinn. *Phys. Rev. B*, 32:5169, 1985.

[13] A. C. Tselis and J. J. Quinn. *Phys. Rev. B*, 29:3318, 1984.

[14] R. Decca, A. Pinczuk, S. Das Sarma, B.S. Dennis, L.N. Pfeiffer and K.W. West, Phys. Rev. Lett. **72**, 1506 (1994).

[15] A. S. Plaut, A. Pinczuk, B.S.Dennis, J.P. Eisenstein, L.N. Pfeiffer and K.W. West, Solid-State Electronics **40**, 291 (1996).

[16] S. Das Sarma and I.K. Marmorkos, Phys. Rev. B **47**, 16343 (1993); I.K. Marmorkos and S. Das Sarma, Phys. Rev. B **48**, 1544 (1993).

[17] S. Ernst, A.R. Goni, K. Syassen and K. Eberl, Phys. Rev. Lett. **72**, 4029 (1994).

[18] A.S. Plaut, A. Pinczuk, P.I. Tamborenea, B.S.Dennis, L.N. Pfeiffer and K.W. West, Phys. Rev. B **55**, 9282 (1997).

[19] J.C. Ryan, Phys. Rev. B **43**, 12406 (1991); D. Gammon, B.V. Shanabrook, J.C. Ryan, D.S.Katzer and M.J. Yang, Phys. Rev. Lett. **68**, 1884 (1992); S.L. Chuang, M.S.C. Luo, S. Schmitt-Rink and A. Pinczuk, Phys. Rev. B **46**, 1897 (1992).

[20] G.F. Giuliani and J.J. Quinn. *Phys. Rev. B*, 31:6228, 1985.

[21] J. W. Wu, P. Hawrylak, and J. J. Quinn. *Phys. Rev. B*, 31:6592, 1985.

[22] V. Piazza, V. Pellegrini, F. Beltram, W. Wegscheider, T. Jungwirth, and A.H. MacDonald. *Nature*, 402:638, 1999.

[23] V. Pellegrini, A. Pinczuk, B.S. Dennis, A.S. Plaut, L.N. Pfeiffer, and K.W. West. *Science*, 281:799, 1998.

[24] G.F. Giuliani and J.J. Quinn. *Surface Science*, 170:316, 1986.

[25] V. Pellegrini, A. Pinczuk, B.S. Dennis, A.S. Plaut, L.N. Pfeiffer, and K.W. West. *Phys. Rev. Lett.*, 78:310, 1997.

[26] S. Das Sarma, Subir Sachdev, and Lian Zheng. *Phys. Rev. Lett*, 79:917, 1997.

[27] E. Demler and S. Das Sarma. *Phys. Rev. Lett*, 82:3985, 1999.

[28] A. H. Macdonald, R. Rajaraman, and T. Jungwirth. *Phys. Rev. B*, 60:8817, 1999.

[29] Min-Fong Yang and Ming-Che Chang. *Phys. Rev. B*, 60:13985, 1999.

[30] E. Demler, Eugene H. Kim, and S. Das Sarma. *Phys. Rev. B*, 61:10567, 2000.

[31] X. M. Chen and J. J. Quinn. *Phys. Rev. Lett.*, 67:895 and 2113, 1991.

[32] H. A. Fertig. *Phys. Rev. B*, 40:1087, 1989.

[33] A. H. MacDonald, P. M. Platzman, and G. S. Boebinger. *Phys. Rev. Lett.*, 65:775, 1990.

[34] L. Brey. *Phys. Rev. Lett.*, 65:903, 1990.

[35] X. M. Chen and J. J. Quinn. *Phys. Rev. B*, 45:11054, 1992.

[36] Y. N. Joglekar and A. H. MacDonald. *Phys. Rev. B*, 65:235319, 2002.

[37] A. Pinczuk, J.P. Valladares, D. Heiman, A.C. Gossard, J.H. English, L. N. Pfeiffer, and K. W. West. *Phys. Rev. Lett.*, 61:2701, 1988.

[38] I. K. Marmorkos and S. Das Sarma. *Phys. Rev. B*, 45:13396, 1992.

[39] C. Kallin and B. I. Halperin. *Phys. Rev. B*, 30:5655, 1984.

[40] S. M. Girvin, A. H. MacDonald, and P. M. Platzman. *Phys. Rev. Lett.*, 54:581, 1985.

[41] S. M. Girvin, A. H. MacDonald, and P. M. Platzman. *Phys. Rev. B*, 33:2481, 1986.

[42] H.D.M. Davies, J.C. Harris, J.F. Ryan, and A. J. Turberfield. *Phys. Rev. Lett.*, 78:4095, 1997.

[43] Moonsoo Kang, Aron Pinczuk, B. S. Dennis, L. N. Pfeiffer, and K. W. West. *Phys. Rev. Lett.*, 86:2637, 2001.

[44] S. Luin, V. Pellegrini, A. Pinczuk, B.S. Dennis, L.N. Pfeiffer, and K.W. West. *Phys. Rev. Lett.*, 90:236802, 2003.

[45] Sudhansu S. Mandal, Michael R. Peterson, and Jainendra K. Jain. *Phys. Rev. Lett.*, 90:106403, 2003.

[46] G. S. Boebinger, H. W. Jiang, L. N. Pfeiffer, and K. W. West. *Phys. Rev. Lett.*, 64:1793, 1990.

[47] M. Kellogg, J.P. Eisenstein I.B. Spielman, L. N. Pfeiffer, and K. W. West. *Phys. Rev. Lett.*, 88:126804, 2002.

[48] L.V. Butov. *Solid State Communication*, 2003. In press.

[49] D. Snoke, Y. Liu, S. Denev, L.N. Pfeiffer, and K.W. West. *Solid State Communication*, 2003. In press.

[50] H.F. Fong, B. Keimer, P.W. Anderson, D. Reznik, F. Dogan, and I.A. Aksay. *Phys. Rev. Lett.*, 75:316, 1995.